A simple method for synthesis of acicular β-Si₃N₄ seed crystals

Daniel A. Gould [a], Mervin Quinlan [a], Maria P. Albano [b], Liliana B. Garrido [b],
Luis A. Genova [c], Kevin P. Plucknett [a,*]

[a] *Materials Engineering Program, Department of Processing Engineering and Applied Science, Dalhousie University, 1360 Barrington Street,
Halifax, Nova Scotia B3J 1Z1, Canada*
[b] *Centro de Tecnología de Recursos Minerales y Cerámica (CETMIC), C.C. 49 (B1897ZCA) M. B. Gonnet, Provincia de Buenos Aires, Argentina*
[c] *IPEN-Instituto de Pesquisas Energéticas e Nucleares, Av. Lineu Prestes 2242, Cidade Universitária, CEP: 05508-000 São Paulo, Brazil*

Abstract

Acicular silicon nitride (β-Si₃N₄) seed crystals have been synthesized using a moderately low temperature heat-treatment process, with the aid of a low volume fraction of multiple sintering aids (i.e. MgO and CaO, in combination with either Y₂O₃ or Nd₂O₃). The effects of the heat-treatment cycle and the additive composition on the α- to β-Si₃N₄ phase transformation were examined, for both cold-isostatically pressed pellets and simple packed powder. In the case of the packed powder, full transformation was achievable following heat-treatment at 1625 °C for four hours, in ~0.1 MPa nitrogen. The use of multiple oxide additives allows seed liberation from the heat-treated materials using a simple dilute HF soak at room temperature. The resulting β-Si₃N₄ seed crystals exhibit a narrow size distribution, with mean aspect ratios of ~4:1.
© 2008 Elsevier Ltd and Techna Group S.r.l. All rights reserved.

Keywords: Silicon nitride; Seed crystals; Heat-treatment; Aspect ratio

1. Introduction

Silicon nitride (Si₃N₄) ceramics are used in a wide variety of engineering applications, for example bearings, cutting tools and turbocharger rotors [1]. As a consequence, there is a significant drive to continually improve the mechanical behavior of Si₃N₄-based materials. In previous work, property improvements have been achieved through either microstructural or compositional design [2–4], or a combination of the two [5]. In particular, it has been demonstrated that development of a bimodal β-Si₃N₄ grain size distribution can favor the formation of high toughness Si₃N₄ ceramics. One approach to the formation of favorable bimodal microstructures involves the use of seeding with β-Si₃N₄ crystals, which grow preferentially, allowing an additional degree of control over microstructural development [2,3,5]. This method has also been applied to porous Si₃N₄, often in combination with a colloidal processing step that allows seed alignment, such as tape casting, although commercial β-Si₃N₄ whiskers have been used in some cases [6].

There have been several reports on the development of techniques to synthesize anisotropic β-Si₃N₄ seed crystals [7–19]. The primary approach that has been taken involves the use of glass forming oxide additives, with seeds generated through the conventional solution–precipitation route that would typically be followed during sintering [7–10,14–19]. These studies have invariably required the use of a high temperature heat-treatment step (i.e. 1700–1850 °C), which is often conducted under a high applied nitrogen pressure to suppress Si₃N₄ decomposition. Alternatively, combustion synthesis approaches have also been demonstrated for the production of β-Si₃N₄ seeds, derived from Si precursors (with α-Si₃N₄ added as a diluent), again using oxide additives to promote the formation of β-Si₃N₄ under high applied nitrogen pressure [11–13]. In these prior studies the selection of sintering additive(s) is such that a highly refractory silicon oxynitride crystalline or glassy phase is formed at the processing temperature, as typically single oxide additions are employed. For example, Hirao and co-workers [7,8] and Ramesh et al. [10] have both used yttria (Y₂O₃) based additions, and required temperatures of 1850 and 1800 °C, respectively, for optimum seed synthesis. Dai et al. produced β-Si₃N₄ seeds with single MgO, Nd₂O₃ or Yb₂O₃ additions at 1650 and 1700 °C [14,15]. However, they

did not subsequently treat the seed grains to remove the additives, and simply prepared them by milling the material after heat-treatment. Hirata et al. heated pure α-Si$_3$N$_4$ powder to 2000 °C, without sintering aids, under elevated nitrogen pressure (~0.9 MPa) [18]. It was observed that elongated β-Si$_3$N$_4$ crystals were formed in a carbon crucible, while equiaxial crystals were formed in a boron nitride crucible. This behavior was attributed to vapor-phase synthesis of β-Si$_3$N$_4$. An extension of the general seed grain synthesis methodology has also allowed the production of α-SiAlON seeds, which can be processed at slightly lower temperatures, although a high nitrogen overpressure was again utilized [16,17].

In the present work a low volume fraction of multiple sintering additives is used, such that β-Si$_3$N$_4$ seed synthesis is possible at 1625 °C. As a consequence of this, a nitrogen overpressure is not required for seed synthesis. The additives used to promote the α- to β-Si$_3$N$_4$ transformation were selected specifically to avoid the formation of β-SiAlON (i.e. no Al$_2$O$_3$). A further major benefit of the present method is that the residual crystalline/glassy phase is readily attacked by dilute HF at room temperature, which makes subsequent separation of the β-Si$_3$N$_4$ seed grains relatively straightforward. Prior studies typically required the use of concentrated HF or H$_3$PO$_4$, often at elevated temperatures, in order to liberate the seed crystals [7–10]. As a consequence, the present method therefore can be seen to be somewhat safer than the majority of prior published techniques for β-Si$_3$N$_4$ seed synthesis.

2. Experimental procedure

All samples in the present work were prepared with Ube SN E-10 α-Si$_3$N$_4$ powder, with 2 wt.% sintering additives (or a molar equivalent). Two additive systems were examined; the first was based on a mixture of 1.5 wt.% Y$_2$O$_3$, 0.25 wt.% MgO and 0.25 wt.% CaO, while the second was identical with the exception that Nd$_2$O$_3$ replaced Y$_2$O$_3$ on a *molar equivalent* basis. Powder mixtures were ball-milled in isopropyl alcohol for 96 h, using tetragonal zirconia (TZP) media; this procedure resulted in a typical milling pick-up of ~3.5 wt.% ZrO$_2$/Y$_2$O$_3$ from the TZP balls [20]. After milling the powders were dried and crushed in a pestle and mortar.

Initial studies focused upon the transformation behavior of the two source powders. Consequently, they were uniaxially pressed into disc-shaped pellets at ~30 MPa, followed by cold-isostatic pressing at ~175 MPa. During sintering the pellets were sited in a powder bed comprised of 50 wt.% α-Si$_3$N$_4$/49 wt.% BN/1 wt.% MgO, and held within a closed high purity graphite crucible. Sintering was conducted at temperatures between 1400 and 1700 °C, for a period of 2 h, in a static nitrogen atmosphere (~800 Torr). For seed grain synthesis the powders were hand-packed into a closed BN crucible (no powder bed was used in this instance), which was itself contained within a closed, high purity graphite crucible. The seed synthesis heat treatments were subsequently performed at temperatures between 1575 and 1625 °C, for a period of 4 h, at a comparable nitrogen pressure to sintering.

The α- to β-Si$_3$N$_4$ phase transformation was characterized by X-ray diffraction (Bruker D-8 Advance, Bruker Inc., Madison, WI), using Cu Kα radiation at a tube voltage of 40 kV. The relative β-Si$_3$N$_4$ content was determined using the method outlined by Yeheskel and Gefen [21]. Seed crystals were obtained by soaking a small portion of the sintered mass in 49% HF acid, diluted 5:1 with doubly distilled water, for a period of 24 h. After soaking the seeds were filtered using a Millipore filter (0.15 μm pore size), and rinsed multiple times with doubly distilled water. To analyze the aspect ratio of the seed crystals they were dispersed in acetone and deposited onto a heated aluminum electron microscopy stub, which results in rapid evaporation of the acetone. The sintered samples and seed crystals were subsequently examined in a field emission scanning electron microscope (FE-SEM; Hitachi S-4700, Hitachi High Technologies, Tokyo, Japan), in order to assess fracture surfaces and grain aspect ratios (through measurement of grain length and width), respectively.

3. Results and discussion

3.1. Preliminary sintering trials

Initial studies were aimed at determination of suitable heat-treatment conditions for obtaining complete α- to β-Si$_3$N$_4$ transformation, and consequently pressed pellets were sintered at temperatures between 1400 and 1700 °C. Fig. 1 demonstrates the effects of sintering temperature on the β-Si$_3$N$_4$ content for both the Y$_2$O$_3$–MgO–CaO and Nd$_2$O$_3$–MgO–CaO additive systems. It can be seen that essentially complete transformation can be achieved through sintering at 1600 °C for a period of 2 h. The influence of temperature on microstructure development is highlighted in Fig. 2 for the Nd$_2$O$_3$–MgO–CaO additive system. Relating these images to Fig. 1, it is clear that a high percentage of α- to β-Si$_3$N$_4$ transformation is achieved after sintering at 1550 °C for 2 h (Fig. 2(a)). The resultant microstructure is highly uniform in appearance, and there is clear evidence of anisotropic β-Si$_3$N$_4$ growth. Increasing the sintering temperature to 1700 °C for 2 h primarily results in

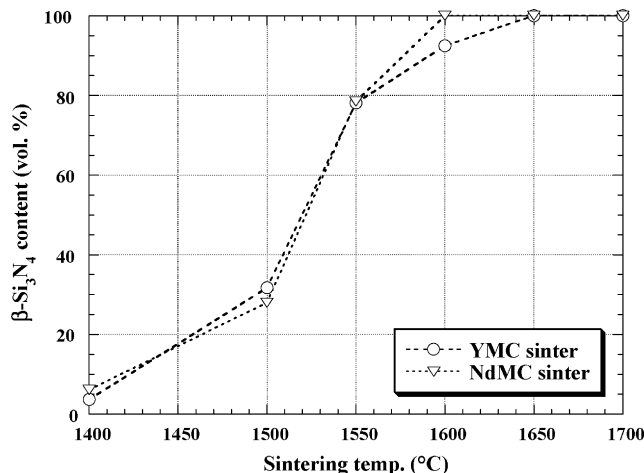Fig. 1. The fraction of β-Si$_3$N$_4$ formed as a function of sintering temperature, determined following the approach of Yeheskel and Gefen [21].

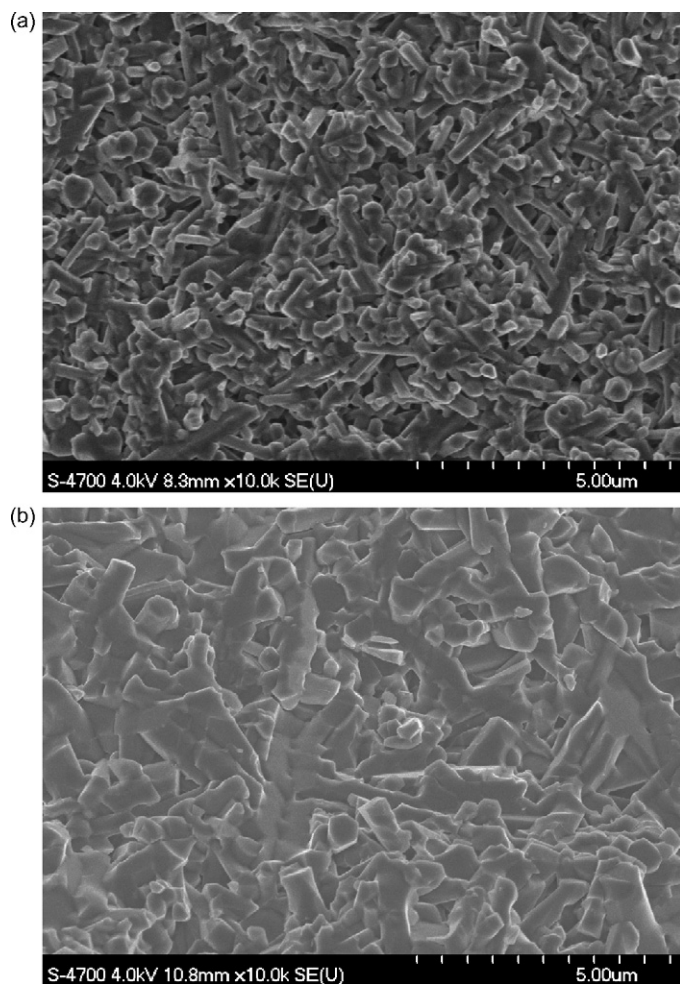Fig. 2. FE-SEM images of fracture surfaces showing microstructural evolution in samples prepared with Nd_2O_3–MgO–CaO additions after sintering for 2 h at (a) 1550 °C and (b) 1700 °C.

coarsening of the microstructure (Fig. 2(b)). It was also apparent that there is appreciable densification of the pellets at the higher sintering temperatures (Fig. 2(b)). Similar studies on the microstructure development of porous β-Si_3N_4 ceramics have shown that milling time can have a strong influence on microstructure development [20]. It has been shown that increasing milling duration leads to a reduction in the β-Si_3N_4 aspect ratio and an increase in densification.

There are several factors that contribute to this behavior. Firstly, the α-Si_3N_4 powder used has an initial β-Si_3N_4 content of $\sim$4 vol.%, which is present in the form of very fine whiskers. Some of these whiskers act as seeds for β-Si_3N_4 growth. Extended duration milling can be expected to reduce the length of these whiskers, and consequently increase their number, therefore creating more potential β-Si_3N_4 nucleation sites. Increasing milling time will also result in size reduction of the α-Si_3N_4 powder, although this effect is actually small, as the starting powder size is $\sim$300–400 nm. Finally, it can be anticipated that there will be some compositional change in the α-Si_3N_4 powder. This will be manifested in two ways: (i) increased SiO_2 content due to increased surface area and (ii) the increasing addition of ZrO_2 (and Y_2O_3) to the starting powder

through wear of the TZP milling media. For the present work, a typical ZrO_2/Y_2O_3 "pick-up" of $\sim$3.5 wt.% was observed during ball milling for 96 h with the TZP media [20].

3.2. β-Si_3N_4 seed preparation

Following the initial assessment of transformation kinetics, seed grain preparation was conducted using a hand-packed powder mixture. In this instance a longer furnace hold was maintained, increasing from 2 to 4 h, as the powders will have a significantly lower packing density in this arrangement ($\sim$20–25% of theoretical). It was observed that complete α- to β-Si_3N_4 transformation was obtained for both the Y_2O_3 and Nd_2O_3-based additive systems after heat-treatment at 1625 °C for 4 h (Fig. 3). The amount of β-Si_3N_4 formed at each heat-treatment temperature is shown in Table 1. At 1600 °C, only the Nd_2O_3–MgO–CaO system showed complete transformation, with $\sim$12 vol.% α-Si_3N_4 retained for the Y_2O_3–MgO–CaO. At 1575 °C, residual α-Si_3N_4 was retained for both compositions, but especially the Y_2O_3-based system where nearly 60% remained. This difference at 1575 °C was attributed to the higher eutectic temperature that can be expected for the Y_2O_3 containing samples [22], combined with the increased diffusion distances in the hand-packed powder. As a consequence, further characterization was restricted to the materials heat-treated at 1625 °C for 4 h. Fig. 4 demonstrates typical β-Si_3N_4 seed crystals extracted using the single stage HF dissolution for both the Nd_2O_3–MgO–CaO and Y_2O_3–MgO–CaO additive systems, after heat-treatment at 1625 °C for 4 h. It is qualitatively apparent that the seed crystals are quite uniform in size and aspect ratio.

In the present work a single stage dissolution treatment was used largely as the seeds are to be utilized in the processing of both porous and dense Si_3N_4-based ceramics prepared with similar additives [22]. An even more extreme "zero-cleaning" approach has been previously assessed by Dai et al., and has been shown to be perfectly suitable when preparing materials based on using identical additives to those for seed preparation [14,15]. However, it is ultimately likely that secondary cleaning stages will be necessary to remove potential fluoride contaminants. It is notable that a major advantage of the present β-Si_3N_4 seed production process is that potentially more dangerous recovery processes can be avoided. For example, previous studies have included treatments in concentrated HF or phosphoric acid (H_3PO_4), often at elevated temperatures [7–10]. Clearly, the use of a dilute HF soak, which can be performed under nominally ambient conditions, presents

Table 1

X-ray diffraction analysis of the nominal β-Si_3N_4 volume fractions as a function of heat-treatment temperature for the Nd_2O_3 and Y_2O_3-based additive systems, determined following the approach of Yeheskel and Gefen [21]

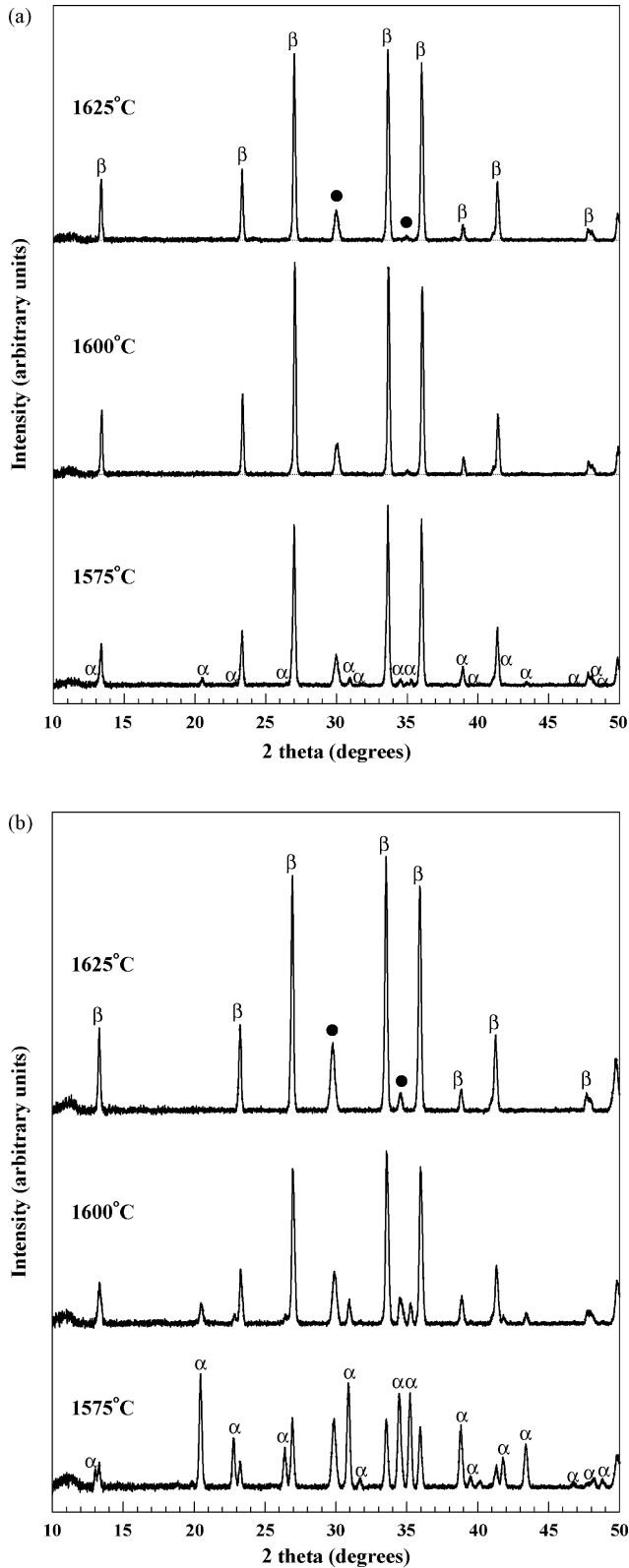| Additives	β-Si_3N_4 content (vol.%)		
	1575 °C	1600 °C	1625 °C
Nd_2O_3–MgO–CaO	96.0	100.0	100.0
Y_2O_3–MgO–CaO	39.5	87.2	100.0

Fig. 3. (a) X-ray diffraction spectra for β-Si$_3$N$_4$ seed crystals produced through heat-treatment at temperatures between 1575 and 1625 °C, for 4 h in ∼0.1 MPa nitrogen, using Nd$_2$O$_3$–MgO–CaO additions. Key: (α) α-Si$_3$N$_4$, (β) β-Si$_3$N$_4$, (●) ZrO$_2$-based phase. (b) X-ray diffraction spectra for β-Si$_3$N$_4$ seed crystals produced through heat-treatment at temperatures between 1575 and 1625 °C, for 4 h in ∼0.1 MPa nitrogen, using Y$_2$O$_3$–MgO–CaO additions. Key: (α) α-Si$_3$N$_4$, (β) β-Si$_3$N$_4$, (●) ZrO$_2$-based phase.
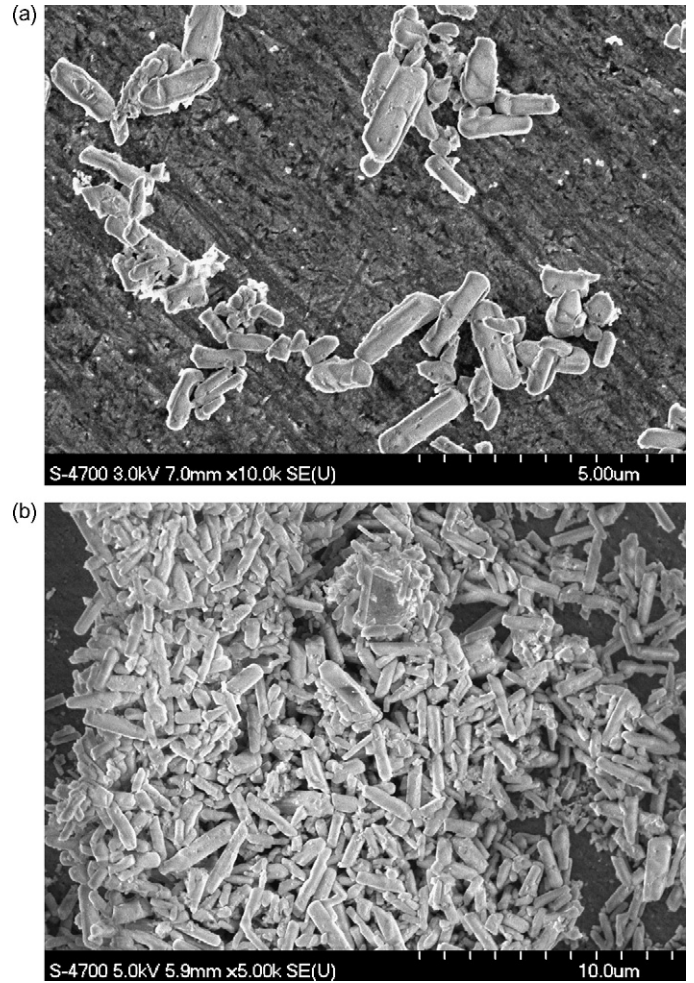
Fig. 4. FE-SEM images of β-Si$_3$N$_4$ seed crystals prepared by heat-treatment at 1625 °C for 4 h, with (a) the Nd$_2$O$_3$–MgO–CaO additive system and (b) the Y$_2$O$_3$–MgO–CaO additive system.

a reduced safety risk when compared to the use of concentrated acids at elevated temperatures, although care must still be taken.

For previous studies that used Y$_2$O$_3$ or other rare earth oxides as transformation aids [7–10], either with or without SiO$_2$, a refractory crystalline intergranular phase can be expected after heat-treatment. For example, based on the Si–Y–O–N system [23], with 2 wt.% Y$_2$O$_3$ (even without additional SiO$_2$) one of the yttrium disilicate (Y$_2$Si$_2$O$_7$) polymorphic phases can be anticipated to form, potentially in combination with small amounts of silicon oxynitride (Si$_2$N$_2$O). Herrmann et al., assessing the corrosion behavior of a variety of dense β-Si$_3$N$_4$ ceramics in H$_2$SO$_4$, noted that materials processed with a crystalline grain boundary phase can exhibit significantly improved resistance to corrosion when compared to materials with a glassy grain boundary phase [24]. Sharkaway and El-Aslabi noted that a β-Si$_3$N$_4$ ceramics HIPed with 2.7 wt.% Y$_2$O$_3$ additions showed better corrosion resistance in HF than a pressureless-sintered material prepared with Y$_2$O$_3$ and Al$_2$O$_3$, while this behavior was reversed during corrosion in HCl [25]. This response was attributed to a passivating phenomenon induced by YF$_3$ precipitation onto the surface of the
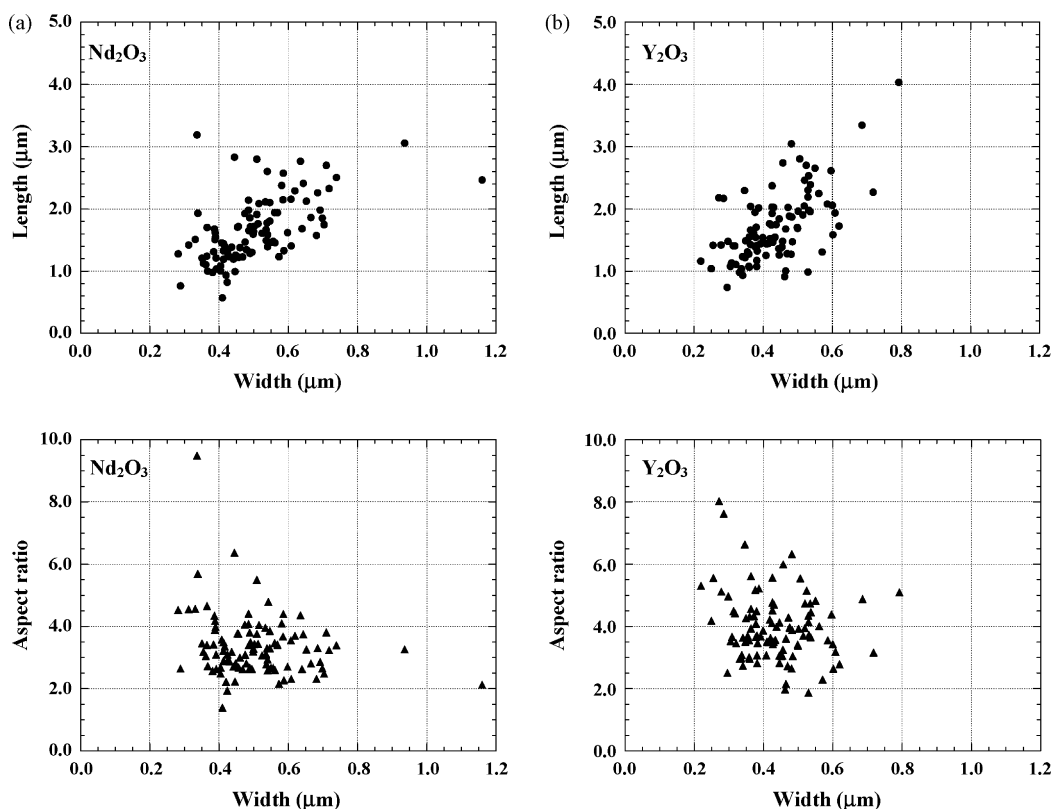
Fig. 5. β-Si$_3$N$_4$ seed grain sizes and aspect ratios for samples prepared by heat-treatment at 1625 °C for 4 h, with (a) the Nd$_2$O$_3$–MgO–CaO additive system, and (b) the Y$_2$O$_3$–MgO–CaO additive system.

pressureless-sintered material, which itself contained a high Y$_2$O$_3$ content at 12.5 wt.%.

In the present work, a Zr-containing crystalline phase is believed to form for both additive systems (Fig. 3). Phase identification for the Nd$_2$O$_3$ containing samples indicates either tetragonal or cubic ZrO$_2$, with a nominal composition of Zr$_{0.9}$Nd$_{0.1}$O$_{1.95}$ (ICCD structure files 86-0334 and 86-0333, respectively); it can be expected that some Mg and Ca may also be incorporated, as they both readily alloy with ZrO$_2$ [26]. The pattern fit for the Y$_2$O$_3$-based additive series is less clear, but again a stabilized ZrO$_2$-based phase is likely; in this instance the best pattern fits are to cubic and rhombahedral ZrO$_2$ (ICCD experimental files 30-1468 and 37-1307, respectively). It is also anticipated that there will be some residual glass in these compositions. Previously it was demonstrated that the dissolution response of SiO$_2$-based oxide glasses in aqueous HF solutions is strongly dependent on the fraction of non-bridging oxygen ions (which determines the glass network connectivity), the concentration of SiO$_2$, the HF concentration in solution and the reaction temperature [27,28]. It can therefore be seen that glass network modifiers such as MgO and CaO will generate increased non-bridging oxygen ions in the silicate structure, thus increasing the glass dissolution rate. Similarly, rare earth oxides such as Y$_2$O$_3$ and Nd$_2$O$_3$ are also proposed to play a network modifying role in oxynitride glass formation [29]. As a consequence, it is clear that the multi-component glass used in the present synthesis method will result in easier liberation

of single grains than for the case of single oxide additions such as Y$_2$O$_3$ or other rare earth oxides [7–10]. However, it is also noted that selected studies have used multi-component additives that incorporate moderate amounts of Al$_2$O$_3$ [19]. In this instance, a β-Si–Al–O–N solid solution alloy can be anticipated, rather than pure β-Si$_3$N$_4$.

As noted above, the multi-cation crystalline/glass phases that are formed during heat-treatment are readily amenable to dissolution in moderately dilute HF. Fig. 5 demonstrates the β-Si$_3$N$_4$ seed crystal dimensions and aspect ratios that have been determined for the two additive systems, following heat-treatment at 1625 °C for 4 h in ~0.1 MPa nitrogen. It is clear that the seeds are of relatively uniform size and shape after the processing cycle that was undertaken. It is important to note that the extended duration milling procedure that was followed results in a general refinement of the grain size and shape, and a move towards a monomodal distribution, rather than a bimodal distribution [20]. It is demonstrated in Fig. 5 that the general seed dimensions and aspect ratios are similar for both Y$_2$O$_3$ and Nd$_2$O$_3$, indicating the choice of rare earth does not play a major role in seed grain development when a low volume fraction multi-component additive system is used. It is notable that with a high volume fraction of sintering additives, the role of the rare earth element becomes more pronounced, such that higher aspect ratios arise with increasing rare earth ionic radius [30]. However, this effect is partially suppressed when the total additive content is relatively small [22]. Table 2 summarizes the mean seed grain dimensions and aspect ratios for both the Y$_2$O$_3$

Table 2
Mean dimensions and aspect ratios for seeds prepared by heat-treatment at 1625 °C for 4 h, using the Nd_2O_3 and Y_2O_3-based additive systems

Additives	Length (μm)	Width (μm)	Aspect ratio
Nd_2O_3–MgO–CaO	1.67	0.50	3.36
Y_2O_3–MgO–CaO	1.71	0.44	3.97

and Nd_2O_3-based additive systems, after heat-treatment at 1625 °C for 4 h.

It can be expected that the formation of seed crystals in the current work will follow the conventional solution-precipitation mechanism of Si_3N_4-based ceramics. In the present case, the use of a 96 h milling step results in a nominally monomodal β-Si_3N_4 grain size after heat-treatment; bimodal grain size distributions are noted for short milling duration treatments of generally similar compositions [20]. The α-to β-Si_3N_4 transformation behavior will be dependent upon the pre-existing β-Si_3N_4 seeds in the starting powder; the Ube SN E-10 α-Si_3N_4 powder typically contains around 4 vol.% β-Si_3N_4, present as extremely fine diameter needles (typically <100 nm diameter) with high aspect ratios (typically >10:1). The extended milling treatment can be expected to reduce the β-Si_3N_4 seed aspect ratio, thus increasing the effective number density of the β-Si_3N_4 particles in the starting powder. Krämer et al. [31] have proposed that a minimum β-Si_3N_4 grain diameter, d_{crit}, is necessary for the ''seed'' particles to be able to grow. Extended duration milling is likely to both *increase* the number of β-Si_3N_4 particles, by breaking high aspect ratio grains into shorter lengths, and possibly slightly *reduce* the grain diameter through mechanical attrition. However, it is proposed that the number of effective grains exceeding d_{crit} is still *increased* in the present case, such that a higher concentration of seed-grains is obtained for heterogeneous nucleation, resulting in a more uniform final grain size and aspect ratio.

4. Summary

The present work has demonstrated a simple procedure to prepare β-Si_3N_4 seed crystals at moderately low processing temperatures. A low volume fraction of combined oxide sintering additives was used to lower the α- to β-Si_3N_4 phase transformation temperature, such that complete transformation could be achieved at ~1600 °C. Fully transformed β-Si_3N_4 seed crystals, with an approximate aspect ratio of 4:1, were subsequently prepared by heat-treatment at 1625 °C for a period of 4 h. A further benefit of this process is that the crystalline/glass intergranular phase that is formed is more amenable to acidic dissolution, such that a 24 h soak at room temperature in dilute HF was sufficient to liberate individual β-Si_3N_4 seed grains.

References

[1] G. Petzow, M.J. Hoffmann, Struct. Bond. 102 (2002) 47–167.
[2] K. Hirao, T. Nagaoka, M.E. Brito, S. Kanzaki, J. Am. Ceram. Soc. 77 (1994) 1857–1862.
[3] H. Imamura, K. Hirao, M.E. Brito, M. Toriyama, S. Kanzaki, J. Am. Ceram. Soc. 104 (1996) 748–751.
[4] A.J. Pyzik, D.R. Beaman, J. Am. Ceram. Soc. 76 (1993) 2737–2744.
[5] P.F. Becher, E.Y. Sun, K.P. Plucknett, K.B. Alexander, C.-H. Hsueh, H.-T. Lin, E.-S. Kang, K. Hirao, M.E. Brito, J. Am. Ceram. Soc. 81 (1998) 2821–2830.
[6] Y. Shigegaki, M.E. Brito, K. Hirao, M. Toriyama, S. Kanzaki, J. Am. Ceram. Soc. 79 (1996) 2197–2200.
[7] K. Hirao, A. Tsuge, M.E. Brito, S. Kanzaki, J. Ceram. Soc. Jpn. 101 (1993) 1078–1080.
[8] M. Kitayama, K. Hirao, M. Toriyama, S. Kanzaki, J. Ceram. Soc. Jpn. 107 (1999) 930–934.
[9] M. Kitayama, K. Hirao, M. Toriyama, S. Kanzaki, J. Ceram. Soc. Jpn. 107 (1999) 995–1000.
[10] P.D. Ramesh, R. Oberacker, M.J. Hoffmann, J. Am. Ceram. Soc. 82 (1999) 1608–1610.
[11] D. Chen, B. Zhang, H. Zhuang, W. Li, S. Xu, J. Inorg. Mater. 17 (2002) 696–702.
[12] D. Chen, B. Zhang, H. Zhuang, W. Li, S. Xu, Mater. Lett. 57 (2002) 399–402.
[13] W. Li, D. Chen, B. Zhang, H. Zhuang, W. Li, Mater. Lett. 58 (2004) 2322–2325.
[14] J. Dai, J. Li, Y. Chen, L. Yang, J. Eur. Ceram. Soc. 23 (2003) 1543–1547.
[15] J. Dai, J. Li, Y. Chen, L. Yang, G. Sun, Mater. Res. Bull. 38 (2003) 609–615.
[16] M. Zenotchkine, R. Shuba, J.S. Kim, I.-W. Chen, J. Am. Ceram. Soc. 84 (2001) 1651–1653.
[17] M. Zenotchkine, R. Shuba, I.-W. Chen, J. Am. Ceram. Soc. 87 (2004) 1040–1046.
[18] T. Hirata, K. Akiyama, T. Morimoto, J. Eur. Ceram. Soc. 20 (2000) 1191–1195.
[19] L.A. Genova, V.A. Izhevskyi, J.C. Bressiani, J. Eur. Ceram. Soc. 28 (2008) 295–301.
[20] M. Quinlan, D. Gould, C. Munro, L. Garrido, L. Genova, K.P. Plucknett, in preparation.
[21] O. Yeheskel, Y. Gefen, Mater. Sci. Eng. 71 (1985) 95–99.
[22] K.P. Plucknett, M. Quinlan, L. Garrido, L. Genova, Mater. Sci. Eng. A 489 (2008) 337–350.
[23] L.J. Gaukler, H. Hohnke, T.Y. Tien, J. Am. Ceram. Soc. 63 (1980) 35–37.
[24] M. Herrmann, J. Schilm, W. Hermel, A. Michaelis, J. Ceram. Soc. Jpn. 114 (2006) 1069–1075.
[25] S.W. Sharkawy, A.M. El-Aslabi, Corr. Sci. 40 (1998) 1119–1129.
[26] R. Stevens, An Introduction to Zirconia, MEL, Twickenham, 1986.
[27] G.A.C.M. Spierings, J. Mater. Sci. 28 (1993) 6261–6273.
[28] D.M. Knotter, J. Am. Chem. Soc. 122 (2000) 4345–4351.
[29] H. Tokunaga, S. Ideguchi, F. Shimizu, N. Saito, K. Nakashima, J. Jpn. Inst. Met. 71 (2007) 445–451.
[30] P.F. Becher, G.S. Painter, N. Shibata, R.L. Satet, M.J. Hoffmann, S.J. Pennycook, Mater. Sci. Eng. A422 (2006) 85–91.
[31] M. Krämer, M.J. Hoffmann, G. Petzow, Acta Metall. Mater. 41 (1993) 2939–2947.